NUMERICAL SIMULATION AND VISUALIZATION OF AIR FLOW IN RANQUE-HILSCH VORTEX TUBE[1]

Anatoliy Khait, Alexander Noskov, Vladimir Alekhin & Aleksey Antipin
Ural Federal University named after the first President of Russia B.N. Yeltsin, Ekaterinburg, Russia

ABSTRACT: *Visualization of air flow which appears in Ranque-Hilsch vortex tube is performed by numerical simulations using different turbulence models. The following turbulence models have been used during computations: k-ε, k-ε Realizable, k-ε RNG, SST and SAS-SST. It was found out that only SAS-SST turbulence model can predict the existence of large-scale secondary vortex structures within the computational domain. The existence of large-scale secondary vortex structures is confirmed by different experimental studies.*

KEYWORDS: *Ranque-Hilsch effect, vortex tube, computational fluid dynamics, CFD, flow visualization*

1. INTRODUCTION

At present time most buildings are equipped with state-of-the-art climate systems allowing maintenance of optimum values of humidity and air temperature within all rooms. In a winter season these systems carry out heating air in a building and in summertime provide its cooling. The principle of operation of such systems is generally based on thermodynamic cycles of coolants and such systems used to be called chillers. The typical coolants are Freon and Ammonia which are not ecological ones. Chillers also have other essential disadvantages such as design complexity, high labor-output ratio and presence of toxic substances. Nevertheless chillers fill all segments of refrigerating machinery in building area despite its disadvantages.

One of the alternative ways of cooling and heating is use of Ranque-Hilsch vortex tubes. Ranque-Hilsch effect arises in the swirled flows of viscous compressed gas (air in particular) and it works in a special device – vortex tube (Piralishvili et al. 2000; Merkulov 1969). Vortex tubes can use atmosphere air in thermodynamic cycle to produce heat flow. Air also can be used as a heat carrier. Vortex tubes are ecologically effective devices; they have very simple design and structure, low labor-output ratio and some other benefits.

In spite of the benefits of vortex tubes the area of their competitiveness is essentially limited due to low power efficiency. The value of isentropic energy efficiency coefficient (IEEC) calculated by equation (Eq. 1) for modern vortex tubes is not higher than 0,4. If this value increases up to 0,8 vortex tubes will be competitiveness in all building areas.

$$\eta_S = \frac{\Delta I_X}{\Delta I_S} \tag{1}$$

where ΔI_x – difference of enthalpies of inlet and cold flows of vortex tube; ΔI_S – difference of enthalpies in the ideal isentropic gas expansion from the inlet flow pressure to cold flow pressure.

Citation: Khait, A., Noskov, A., Alekhin, V. & Antipin, A. (2013). Numerical simulation and visualization of air flow in Ranque-Hilsch vortex tube. In: N. Dawood and M. Kassem (Eds.), Proceedings of the 13th International Conference on Construction Applications of Virtual Reality, 30-31 October 2013, London, UK.

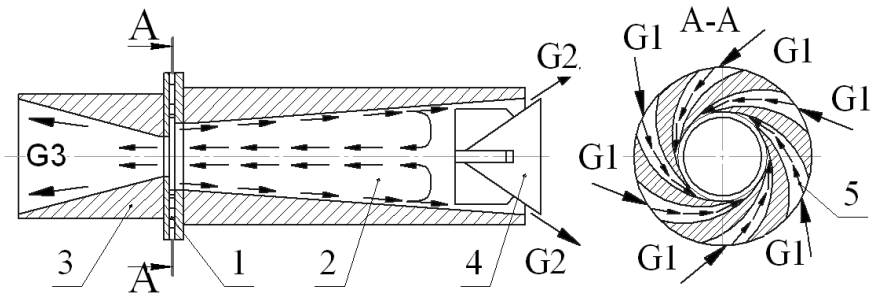

Fig. 1: Schematic diagram of vortex tube. 1- Nozzle inlet; 2 – Vortex energy separation chamber; 3 – Cold flow diffuser; 4 – Hot part cross; 5 –Nozzle duct. G1 – Main compressed gas flow inlet; G2 – Hot flow outlet; G3 – Cold flow outlet

In the simplest case vortex tube is a cylindrical or conical tube which has tangential nozzle inlet for compressed gas (usually air) (fig. 1). Compressed gas is injected into the energy separation chamber passing through the nozzle inlet, and it forms the vortex flow. Outer part (part placed near the wall) of the vortex flow has higher total temperature in compare with inlet gas. Central part of the flow has lower total temperature. Cold and hot gases flow out from different sides of the vortex tube (Piralishvili et al. 2000; Merkulov 1969).

Many researchers (Hilsch 1947; Skye et al. 2006; Selek et al. 2010; Behera et al. 2005; Dincer et al. 2010; Farouk et al. 2007; Dutta et al. 2010; Chang et al. 2011; Lovtsov et al. 2011; Khait et al. 2012) have made different attempts to improve the design of modern vortex tubes in order to increase its IEEC. The conventional approach in the research is to carry out many experimental measurements using large number of various designs and internal structures of vortex tube elements (Hilsch 1947; Selek et al. 2010; Dincer et al. 2010; Chang et al. 2011). In addition many researchers did not make preliminary calculations of vortex tube geometry elements due to complexity of such calculations.

Despite the large number of experimental investigations performed since 1940s when first industrial vortex tube was engineered the energy efficiency of these devices was not change much. It is caused by very complex structure of hydrodynamic processes appearing in vortex flow of compressible gas. An experimental investigation of these processes is also very limited due to low accuracy of existing measuring tools. Up to the present time there is no sufficient theory of energy separation mechanism. Nomination of necessary sizes of industrial vortex tubes is carried out by the empirical dependences received from experimental data of different researches.

In order to understand the main physical principles of Ranque-Hilsch energy separation effect it is necessary to study internal structure of arising vortex gas flow carefully. Carrying out any experimental studies is significantly complicated. It is caused by high velocities of gas and small geometry sizes of a vortex tube. Introduction of any measuring sensors into the vortex tube leads to gas flow distortion. Active using the computer technologies for simulation and visualization of gas flow arising in vortex tubes for the subsequent analysis is caused by such experimental study complexity.

Numerical simulation makes it possible to get preliminary information concerned hydrodynamics of flows appearing in vortex tubes. There are a lot of publications concerned different attempts of 3D vortex gas flow simulation (Skye et al. 2006; Behera et al. 2005; Farouk et al. 2007; Dutta et al. 2010; Lovtsov et al. 2011; Khait et al. 2012). But the practical application of created numerical models for vortex tube elements design optimization can be found not very often (Behera et al. 2005; Khait et al. 2012). First of all to solve this problem we need high performance computers for running numerical simulations. In the second there is some distrust to results of such computations. Many researchers note the existence of divergences between results of numerical computations and experimental measurements.

The turbulence model is a key option in the numerical simulations. Semi empirical turbulence models (k-ε, k-ω, SST etc.) (Wilcox 1994; Ferziger et al. 2002; Menter 2009) give significant divergence during Ranque-Hilsch energy separation effect simulation. For example Skye (Skye et al. 2006) received divergence of the IEEC value about 40 % in compare with experimental data. Farouk (Farouk et al. 2007) used large eddy simulation turbulence model (LES) for simulation of energy separation effect. It was found that application of LES model allows to

improve some reliability of data obtained by computations but does not solve the problem completely. Development of turbulence model which allows receiving more adequate structure of vortex gas flow is very important task.

In the paper the visualization of air flow appearing in Ranque-Hilsch vortex tube received by numerical simulations using different turbulence models is presented. The analysis of air flow received by Scale adaptive turbulence model (SAS-SST) (Menter 2009) is performed.

2. NUMERICAL MODEL

The numerical model of gas flow based on Reynolds equations was used for undertaking numerical simulations (Loytsyanskiy 2003):

Momentum equation

$$\rho \frac{dV}{dt} = -grad\left(p + \frac{2}{3}\mu_{\Sigma} divV \right) + 2Div(\mu_{\Sigma} \dot{S}) \tag{2}$$

where ρ – density; V – velocity; p – static pressure; $\mu_{\Sigma} = \mu + \mu_t$, μ – molecular viscosity coefficient, μ_t – turbulence viscosity coefficient; $\dot{S}$ – deformation velocities tensor.

Continuity equation

$$\frac{\partial \rho}{\partial t} + div(\rho V) = 0 \tag{3}$$

Energy conservation equation

$$\frac{\partial}{\partial t}(\rho H) + div(\rho V H) - div\left(\frac{\lambda_t}{c_p} grad(h) \right) = \frac{\partial}{\partial t} p \tag{4}$$

where H – total enthalpy; h – static enthalpy; $\lambda_t / c_p = \mu_t / Pr_t$ – turbulence thermal conductivity coefficient; $Pr_t = 0.8$ – turbulent Prandtl number for air; c_p – heat capacity.

Equation of ideal gas state

$$p = \rho R T \tag{5}$$

where R – gas constant

The following turbulence models have been used during computations: k−ε, k−ε Realizable, k − ε RNG, SST and SAS-SST. The application of more complicated turbulence models including Large Eddy Simulation (LES) and Detached Eddy Simulation (DES) leads to significant increase of computational mesh cells number. Both ANSYS and OpenFOAM have been used to solve numerically the mathematical model equations.

The grid independence study has been performed for both k−ε and SAS-SST turbulence models because these models have fundamental distinctions. It was found out that in the case under consideration grid coarseness do not have strong influence on the value of IEEC (1) if the number of grid cells is higher than 500 000. The finest considered grid was consisted of 2,5 million cells. This observation is in agreement with the results of grid independence study performed by (Dutta et al. 2010). The grid consisting of 750 000 cells was used in further computations.

The wall treatment was performed by wall function method. Such wall treatment can be used for simulation of Ranque-Hilsch energy separation phenomenon because the boundary layers do not have significant influence on energy separation in vortex tube. Energy separation is caused basically by heat exchange between outside layers of the swirled flow moving in the direction of hot flow outlet and central layers moving counter flow in the direction of cold outlet. Dimensionless thickness of the grid boundary layer was in the range of $y^+ = 10 – 200$. This grid resolution can be used in couple with wall function treatment (Menter 2009).

Vortex tube computational domain is depicted in fig. 2. Main geometry sizes of computational vortex tube domain: energy separation chamber diameter D = 16,8 mm; diaphragm diameter d = 9,8 mm; energy separation chamber length and conical angle: L = 168 mm, α = 3,5° (fig. 1).

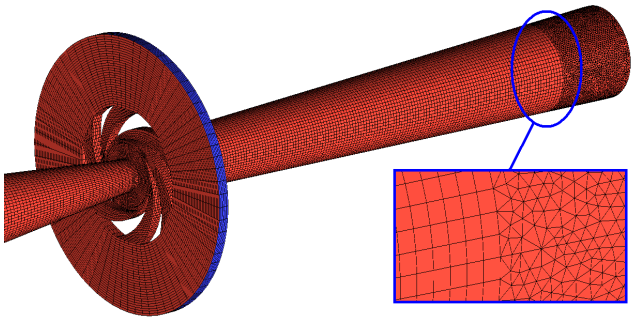

Fig. 2: Vortex tube computational domain

The following initial conditions were used: absolute static pressure $p = 10^5$ Pa; static temperature T = 300 K; velocities $U_x = U_y = U_z = 0$; turbulence kinetic energy k = 0; turbulence dissipation rate ε = 0. The air was used as a continuum; its properties were accounted for by ideal gas state equation (Eq. 5).

Boundary conditions:

- Vortex tube inlet (flow G1, fig. 1): absolute static pressure $p = 5 \cdot 10^5$ Pa; static temperature T = 300 K, turbulence intensity I = 5%.

- Hot flow outlet (G2, рис. 1): absolute static pressure $p = 2{,}6 \cdot 10^5$ Pa. The given value of static pressure was chosen in order to obtain the cold mass flow fraction value (Eq. 6) φ = 0,6.

- Cold flow outlet (G3, fig. 1): absolute static pressure $p = 10^5$ Pa.

- No slip and adiabatic wall boundary conditions were used for all other boundary surfaces.

$$\varphi = G3/G1 \tag{6}$$

where G3 – cold mass flow rate; G1 – inlet mass flow rate.

Computations were carried out in transient formulation. Considered physical time in computations was $t = 2 \cdot 10^{-2}$ s. Achievement of a stationary state of the air flow was detected by monitoring of mass flow rate values in all inlets and outlets of the vortex tube computational domain.

The following solver parameters were used:

- Time integration step: adaptive in the range $\Delta t = 10^{-5}$ - 10^{-7} s.

- Second order scheme for time integration.

- High order scheme for space integration.

3. COMPUTATIONAL INTEGRAL CHARACTERISTICS OF VORTEX TUBE

Performed numerical simulations make it possible to calculate values of IEEC (Eq. 1). Main results of these calculations received using different turbulence models are presented in table 1. It is clear that the most adequate turbulence model showed IEEC value $\eta_S = 0{,}24$. All other turbulence models give very close value of IEEC. At the same time experimental value of this coefficient is about $\eta_S = 0{,}36$ (Lovtsov et al. 2011). This distinction can be caused by inaccuracy of used turbulence models.

Table 1: Isentropic energy efficiency coefficient values for different turbulence models.

No.	Turbulence model	Computational cold mass flow fraction	Cooling degree, $\Delta T = T_{INLET} - T_{COLD}$, K	Isentropic energy efficiency coefficient (IEEC)
1	k - ε	0,59	23,3	0,21
2	k – ε Realizable	0,58	26	0,24

3	k – ε RNG	0,73	24,4	0,22
4	SST	0,58	24,3	0,22
5	SAS-SST	0,64	21,7	0,2

4. VISUALIZATION OF VORTEX AIR FLOW

The visualization of vortex air flow appearing in Ranque-Hilsch vortex tube is made on the basis of results of performed simulations.

4.1 k-ε turbulence model

It was found out that k−ε, k−ε Realizable, k − ε RNG and SST turbulence models predicted very similar flow structure and distribution of main hydrodynamic characteristic within computational domain. That is why the results only for k−ε turbulence model are presented in the paper. Computational distribution of hydrodynamic parameters in the longitudinal vortex tube cross section is presented in fig. 3, 4, 5, 6.

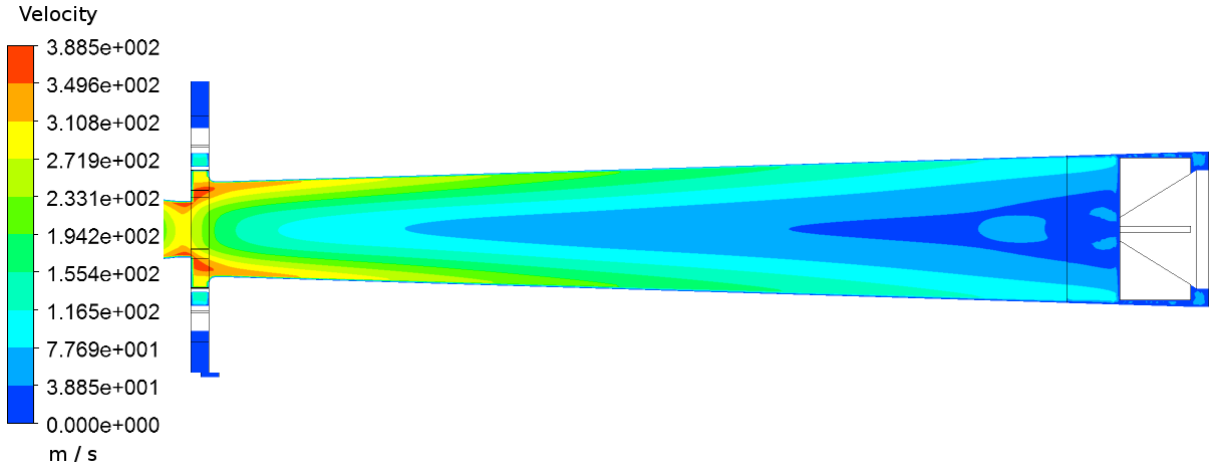

Fig. 3: Distribution of velocity in longitudinal vortex tube cross section

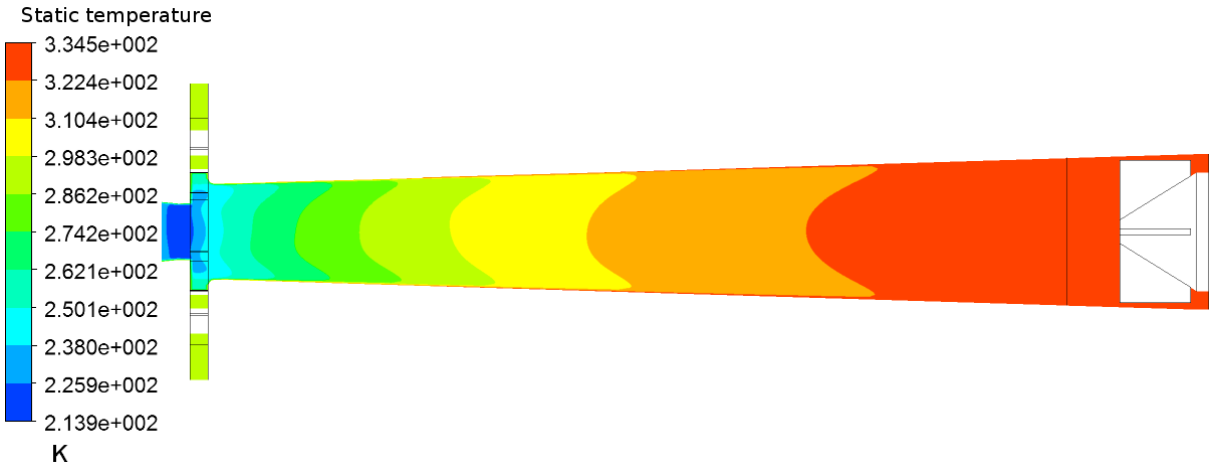

Fig. 4: Distribution of static temperature in longitudinal vortex tube cross section

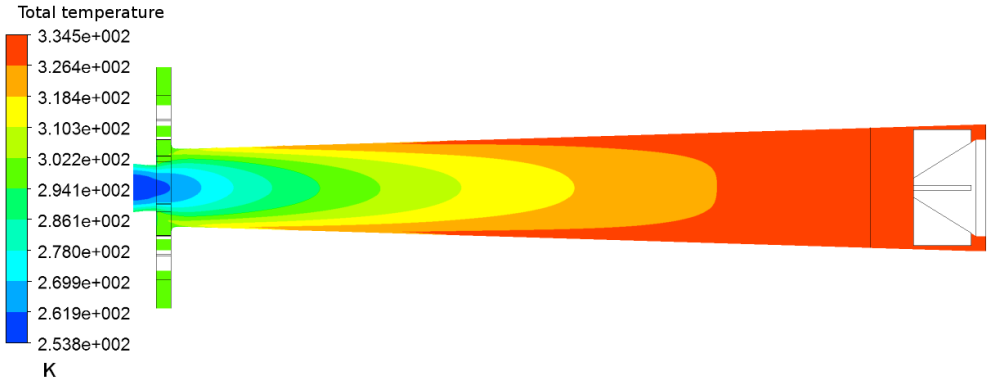

Fig. 5: Distribution of total temperature in longitudinal vortex tube cross section

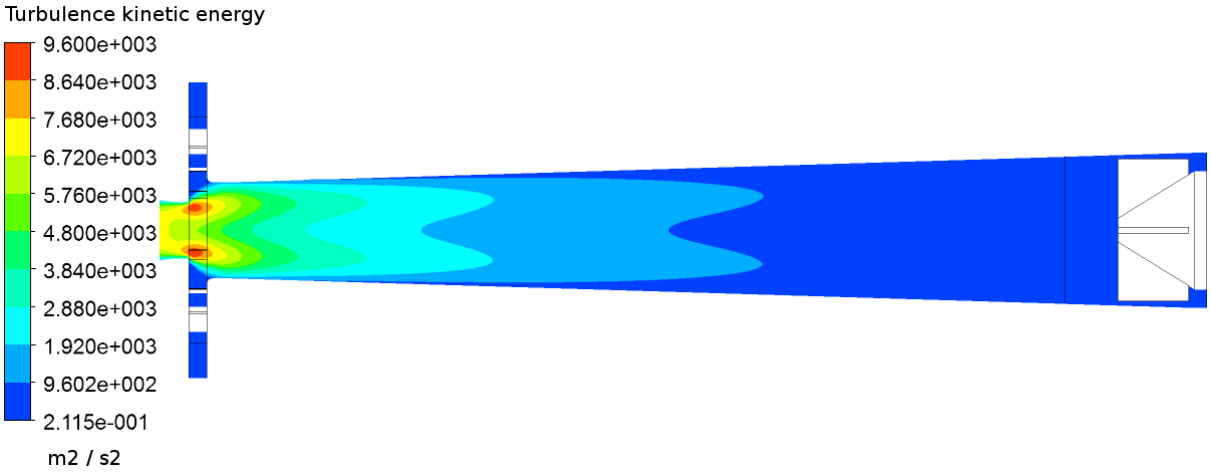

Fig. 6: Distribution of turbulence kinetic energy in longitudinal vortex tube cross section

An analysis of static pressure distribution showed existence of radial pressure gradient which is caused by air flow swirling. Central part of vortex air flow has higher value of static temperature comparing with outer flow part (fig. 4). In the same time total temperature distribution has the opposite tendency (fig. 5). The vortex flow outer part has higher total temperature in compare with the central flow part. This phenomenon can be explained by velocities distribution (fig. 3). The outer part of the vortex flow has the higher value of velocities.

Computational streamlines are presented in fig. 7. The air flow is axisymmetric and stationary.

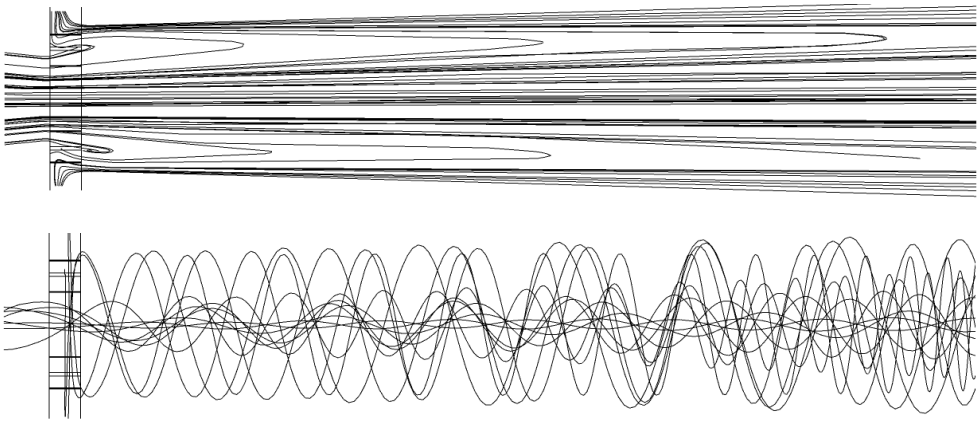

Fig. 7: Computational streamlines in vortex tube found by k-ε turbulence model

4.2 SAS-SST turbulence model

SAS-SST turbulence model shows the structure of appearing vortex flow very different from all other used turbulence models. It can be explained by the fact that this model partially takes into account nonstationarity of turbulence (Menter 2009).

The computational flow structure received by SAS-SST turbulence model shows nonstationary character of the vortex flow. All hydrodynamic parameters undergo continuous pulsation change within the vortex tube computational domain. Distributions of the velocity, static temperature and turbulent kinetic energy in the longitudinal vortex tube cross section are presented in fig. 8, 9 and 10.

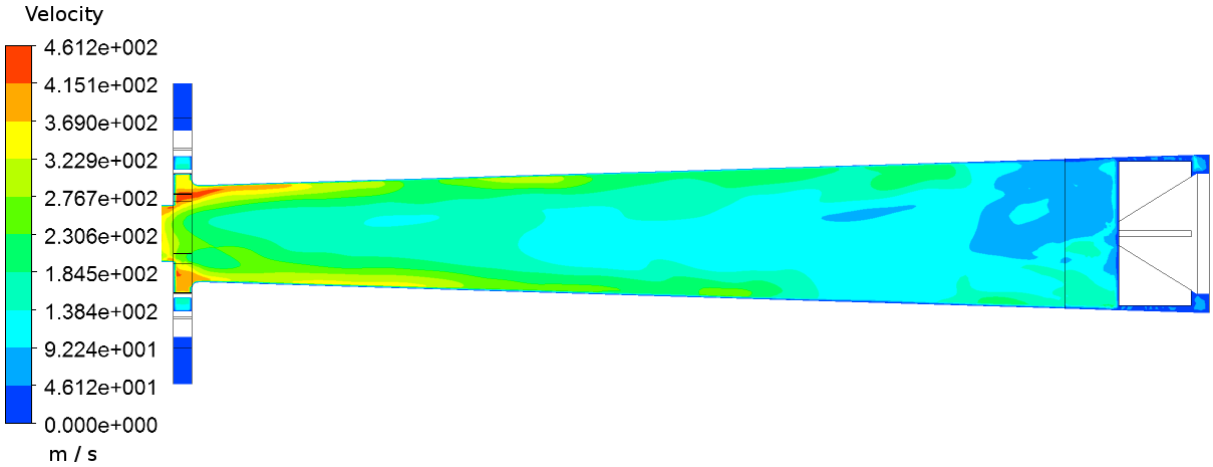

Fig. 8: Distribution of velocity in longitudinal vortex tube cross section

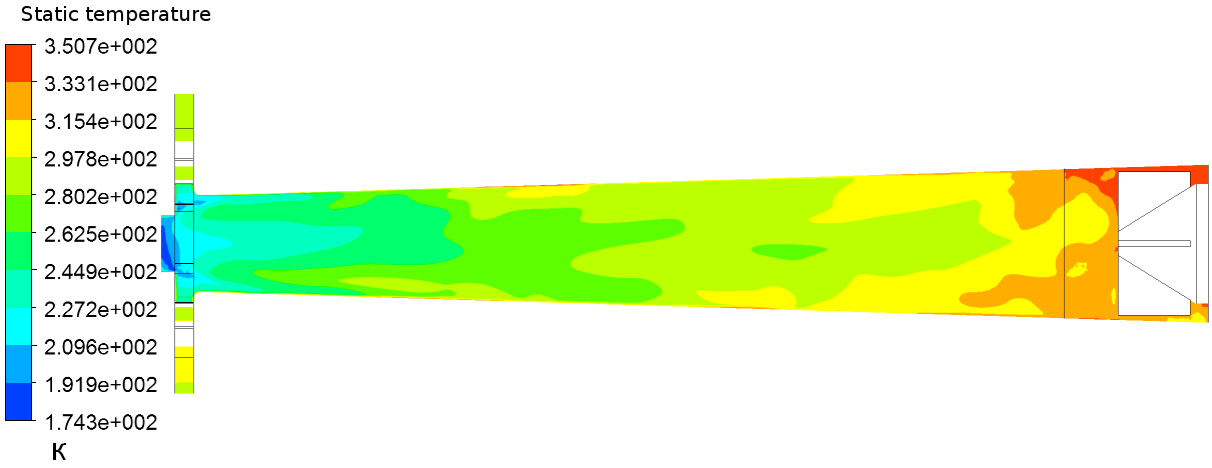

Fig. 9: Distribution of static temperature in longitudinal vortex tube cross section

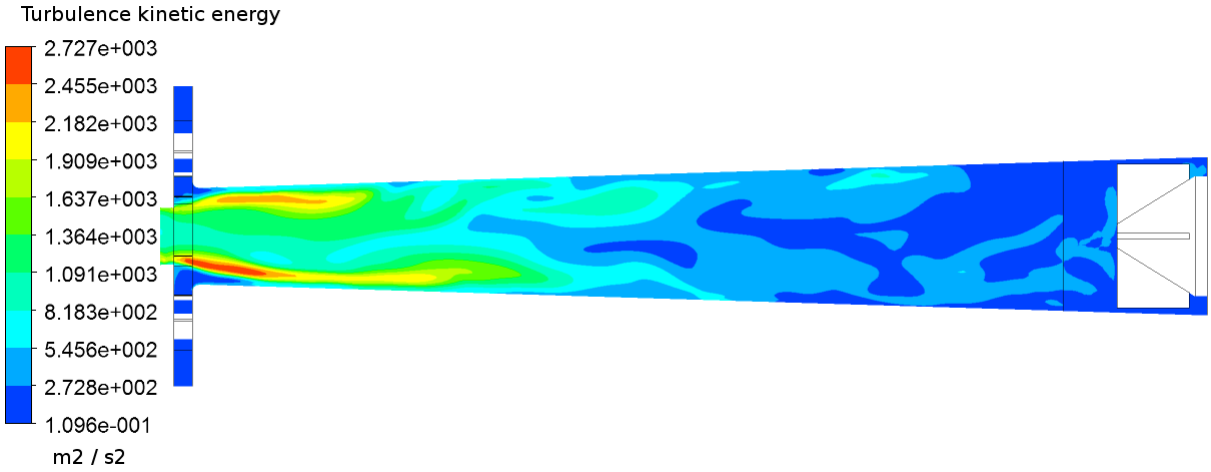

Fig. 10: Distribution of turbulence kinetic energy in longitudinal vortex tube cross section

The flat streamlines within the vortex tube computational domain are presented in fig. 11 in order to visualize the air flow predicted by SAS-SST turbulence model. Unlike a case of application of standard k−ε turbulence model the resulted vortex flow is asymmetric. Also there is a precession of central flow part.

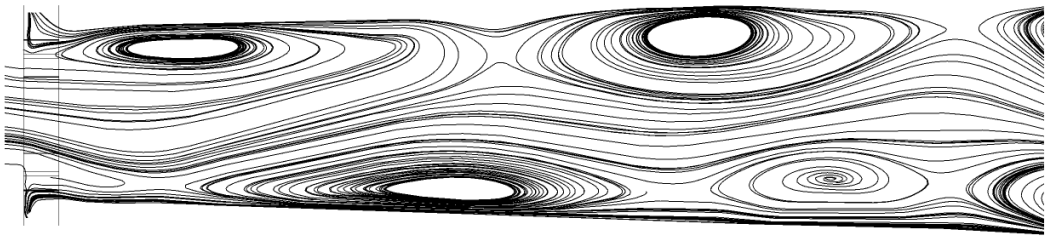

Fig. 11: Flat computational streamlines in vortex tube found by SAS-SST turbulence model

Presented flow visualization makes it possible to find out the existence of vortex structures between central and outer flows. All other used turbulence models do not predict these vortex structures. In the case of application of SAS-SST turbulence model vortex structures fill the entire vortex tube energy separation chamber. In 3D visualization these structures compose continues large-scale secondary vortexes. The existence of such vortexes has been found in some experimental visualization.

Arbuzov (Arbuzov et al. 1997) experimentally study the air vortex flow in square channel where the Ranque-Hilsch effect arises. The method of optical density phase field visualization has been used. The real time visualization of vortex flow has been made using this optical method. Minimum exposition time was 250 ms. Existence of two large-scale secondary vortex structures was found out (fig. 12).

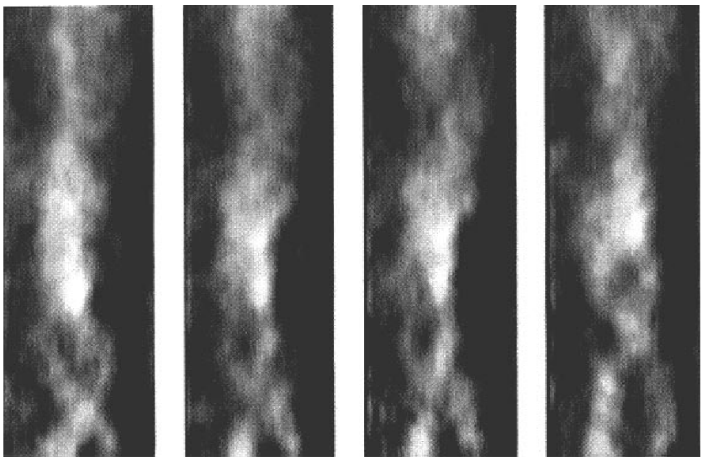

Fig. 12: Experimental large-scale secondary vortex structures optical visualization (Arbuzov et al. 1997)

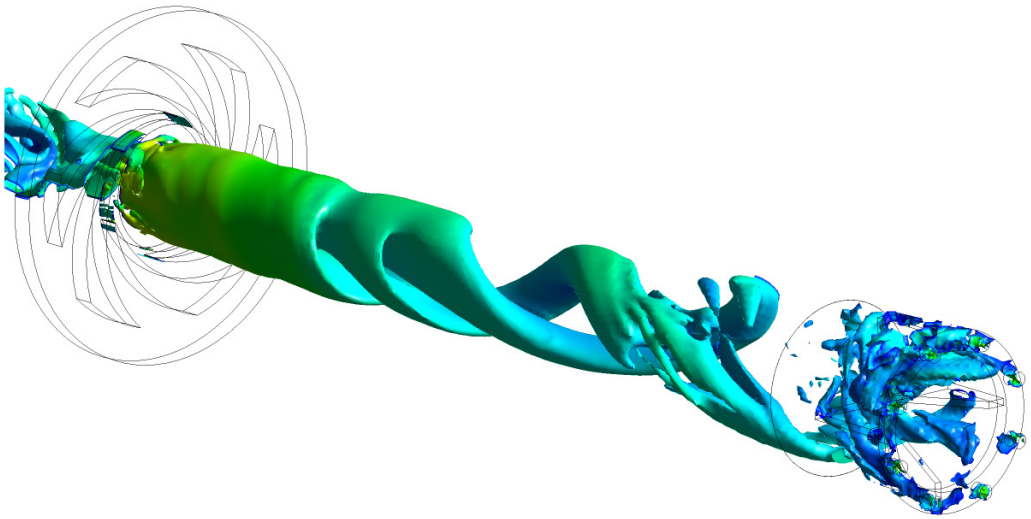

Fig. 13: 3D visualization of large-scale secondary vortex structures in vortex tube received by SAS-SST turbulence model and "vortex core region" algorithm (stream surfaces)

The "vortex core region" algorithm of ANSYS was used to visualize large-scale secondary vortex structures (fig. 13). Three dimensional streamlines are presented in fig. 14. The visualization has very close qualitative agreement with experimental results presented in fig. 12. As a result of visualization we can conclude that SAS-SST turbulence model makes it possible to predict vortex flow structure more precisely unlike other above observed semi empirical turbulence models (k-ε, SST etc.).

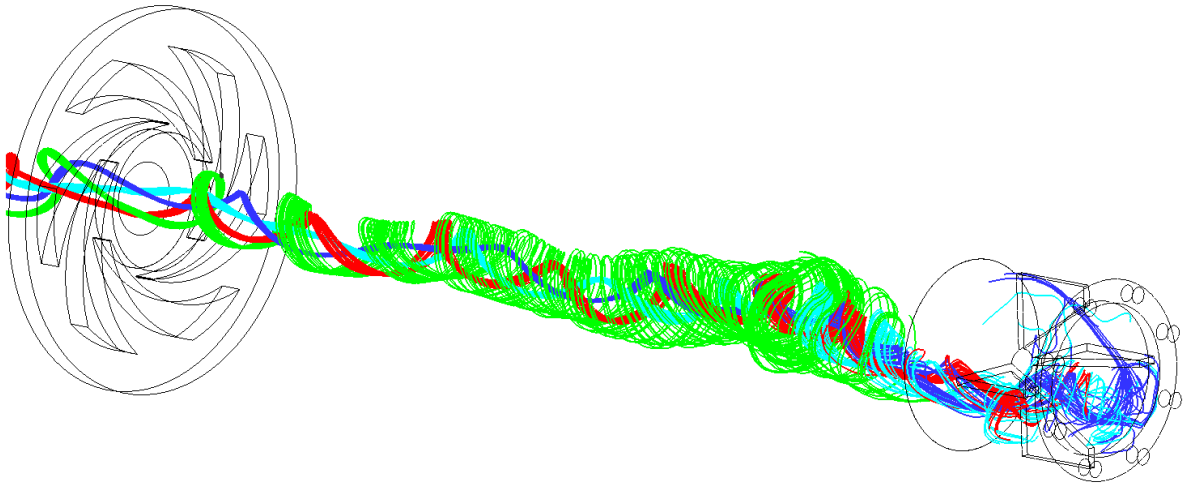

Fig. 14: 3D streamlines in vortex tube received by SAS-SST turbulence model.

5. CONCLUSION

Analysis of vortex tube integral characteristics shows that the isentropic energy efficiency coefficient (IEEC) has the same value for all turbulence models which were under consideration in the paper. The most adequate turbulence model shows IEEC value $\eta_S = 0{,}24$. The experimental value of this coefficient is about $\eta_S = 0{,}36$. This distinction can be caused by inaccuracy of turbulence models. The SAS-SST turbulence model does not increase the accuracy of IEEC prediction but makes it possible to get much more accurate internal structure of appearing vortex air flow.

The visualization of internal structure of appearing vortex flow showed that k−ε, k−ε Realizable, k − ε RNG and SST turbulence models predict very similar flow structure. At the same time SAS-SST turbulence model shows the structure of vortex flow very different from all other used turbulence models. It can be explained by the fact

that this model partially takes into account nonstationarity of turbulence. Only SAS-SST turbulence model predict the existence of large-scale secondary vortex structures within the computational domain. The existence of such vortex structures is confirmed by different experimental studies.

SAS-SST turbulence model can be recommended for further simulations intended for vortex tube energy efficiency improvement because this model allows more accurate prediction of the vortex air flow. If the vortex tube energy efficiency increases up to corresponding values then this device will be competitive in all building and construction areas.

6. ACKNOWLEDGEMENTS

Authors thank A.V. Lovtsov for important remarks and discussions of research results. Partial financial support of presented study by Ural Research and Design Institute of Russian Academy of Architecture and Construction Sciences is gratefully acknowledged.

7. REFERENCES

Arbuzov V. A., Dubnischev Yu. N., Lebedev A. V., Pravdina M. H. and Yarovskiy N. I. (1997). Observation of large-scale hydrodynamic structures in vortex tube and Ranque effect, *JTF letters*, Vol. 23, No. 23, 84-90.

Behera U., Paul P. J., Kasthurirengan S., Karunanithi R., Ram S. N., Dinesh K. and Jacob S. (2005). CFD analysis and experimental investigations towards optimizing the parameters of Ranque–Hilsch vortex tube, *International journal of heat and mass transfer*, No. 48, 1961-1973.

Chang K., Li Q. and Zhou G. (2011). Experimental investigation of vortex tube refrigerator with a divergent hot tube, *International journal of refrigeration*, No. 34, 322-327.

Dincer K., Avci A., Baskaya S. and Berber A. (2010). Experimental investigation and energy analysis of the performance of a counter flow Ranque-Hilsch vortex tube with regard to nozzle cross-section areas, *International journal of refrigeration*, No. 33, 954-962.

Dutta T., Sinhamahapatra K. P. and Bandyopdhyay S. S. (2010). Comparison of different turbulence models in predicting the temperature separation in a Ranque–Hilsch vortex tube, *International journal of refrigeration*, No. 33, 783-792.

Farouk T. and Farouk B. (2007). Large eddy simulations of the flow field and temperature separation in the Ranque–Hilsch vortex tube, *International journal of heat and mass transfer*, No. 50, 4724–4735.

Ferziger J. H. and Peric M. (2002). Computational methods for fluid dynamics, 3rd edition, *Springer*, 423.

Hilsch R. (1947). The use of expansion of gases in a centrifugal field as a cooling process, *Rev. Sci. Instrum.*, No. 18(2), 108-113.

Khait A., Noskov A., Alekhin V. and Lovtsov A. (2012). Mathematical simulation of Ranque-Hilsch vortex tube heat and power performances, *Proceedings of 14th International conference on computing in civil and building engineering*, Moscow, 160-161.

Lovtsov A. V., Noskov A. S. and Khait A. V. (2011). Optimization of vortex forming device used in Ranque-Hilsch vortex tubes, *Proceedings of 4th international conference on Heat and mass transfer and hydrodynamics in swirling flows*, Moscow Power Engineering Institute, 282-283.

Loytsyanskiy L. F. (2003). Liquid and gas mechanics, *Moscow, Drofa*, 840.

Menter F. R. (2009). Review of the shear-stress transport turbulence model experience from an industrial perspective, *International journal of computational fluid dynamics*, Vol. 23, No. 4, 305-316.

Merkulov A. P. (1969). Vortex effect and its application in technique, *Moscow, Mechanical engineering*, 184.

Piralishvili Sh. A., Polyaev V. M. and Sergeev M. N. (2000). Vortex effect. Experiment, theory, technical solutions, *Moscow, Energomash*, 415.

Selek M., Tasdemir S., Dincer K. and Baskaya S. (2010). Experimental examination of the cooling performance of Ranque-Hilsch vortex tube on the cutting tool nose point of the turret lathe through infrared thermography method, *International journal of refrigeration*, doi:10.1016/j.ijrefrig.2010.11.008, 1-9.

Skye H. M., Nellis G. F. and Klein S. A. (2006). Comparison of CFD analysis to empirical data in a commercial vortex tube, *International journal of refrigeration*, No. 29, 71–80.

Wilcox D. C. (1994). Turbulence modeling for CFD, *DCW industries Inc.*, California, 560.